Journal of Mammalogy, 97(1):1–13, 2016
DOI:10.1093/jmammal/gyv146
Published online September 23, 2015

Genetic landscape with sharp discontinuities shaped by complex demographic history in moose (*Alces alces*)

Lovisa Wennerström,* Nils Ryman, Jean-Luc Tison, Anna Hasslow, Love Dalén, and Linda Laikre

Department of Zoology, Division of Population Genetics, Stockholm University, SE-10691 Stockholm, Sweden (LW, NR, AH, LL)
Department of Bioinformatics and Genetics, Swedish Museum of Natural History, SE-10405 Stockholm, Sweden (J-LT, LD)

Present address of AH: Swedish Agency for Marine and Water Management, Box 11930, SE-404 39 Gothenburg, Sweden.

* *Correspondent: lovisa.wennerstrom@zoologi.su.se*

The moose (*Alces alces*) is the most intensely managed game species in Fennoscandia; approximately one-third of the population, ca. 160,000 animals, is harvested annually. Despite the species' biological and socioeconomic importance, there are knowledge gaps with respect to its intraspecific diversity and genetic structure. Recent studies of moose in neighboring countries report 2 genetic groups in Finland, 3 in Norway with one of them suggested to be of ancient origin, and no indications of bottlenecks. To delineate the spatial genetic landscape of the Swedish moose, we used allozyme variability from over 20,000 georeferenced moose collected all over Sweden in combination with 12 microsatellites ($n > 1{,}200$) and mitochondrial DNA (mtDNA) sequences ($n = 44$). We combined individual-based and traditional statistical approaches with coalescence-based simulations. The results indicate a complex history with bottlenecks and recent expansions that is consistent with historical records. Swedish moose are separated into 2 major genetic groups, a northern and a southern one, where the southern group is further divided into 3 subgroups. The 2 main subpopulations are moderately differentiated ($F_{ST} = 0.1$; $R_{ST} = 0.07$) and separated by sharp genetic discontinuities occurring over a relatively narrow transition zone in central Sweden that coincides with a similar, previously reported transition zone in Norway. This differentiation is not reflected in mtDNA variation, where no significant divergence was observed. Together with the F_{ST} and R_{ST} similarities, this suggests that the 2 major subpopulations in Sweden reflect divergence shaped after the postglacial recolonization of Scandinavia. Neighborhood size assessments indicate that gene flow is relatively restricted with an estimated average dispersal distance of 3.5–11.1 km, and spatial autocorrelograms suggest that genetic similarity decreases almost linearly over space resulting in continuous genetic clines within major subgroups. Management areas largely coincide with genetic clusters, simplifying the integration of genetic information into management.

Key words: approximate Bayesian computation, population genetic structure, spatial autocorrelation, wildlife management

Population genetic structure constitutes basic biological information of relevance for both understanding species' evolutionary history and for their conservation and long-term persistence. For species that are subjected to large-scale human influence, such as hunting and fishing, population genetic data are needed for sustainable management (Laikre and Ryman 1996; Allendorf et al. 2008; Laikre et al. 2008). The moose (*Alces alces*) is a species of high socioeconomic and ecological importance in northern Europe for which several population genetics questions remain unanswered. Over the last century, and particularly from the 1950s and onwards, the moose has recovered from being severely threatened to becoming extremely abundant over Fennoscandia where the populations have reached almost one-half million animals, with about one-third being harvested annually in Norway, Sweden, and Finland (Luoma 2002; Solberg et al. 2005, 2006; Swedish Association for Hunting and Wildlife Management 2008; Åkesson 2009; Nygrén 2009). Our study includes investigating the potential existence of genetic signatures of this recent dramatic demographic history for moose over Sweden for which much less is known than for the rest of Fennoscandia.

The moose has been part of the Fennoscandian fauna since the retreat of the ice sheet at the end of the last glaciation ca. 7,000–9,000 years ago (Strandgaard 1982). Colonization of this area from various glacial refugia has taken different routes for different species (Taberlet et al 1998). Typically, species have colonized the Scandinavian Peninsula either from the south (e.g., meadow grasshopper *Chorthippus parallelus* and hedgehog *Erinaceus europaeus*—Szymura et al 1996; Seddon et al 2002; Hewitt 2011), from the north (e.g., Norway spruce *Picea*

abies—Schmidt-Vogt 1977), or from both north and south (e.g., brown bear *Ursus arctos*—Taberlet and Bouvet 1994; Taberlet et al. 1998). It has been suggested that moose colonized Fennoscandia from both the south and the north; Sweden being colonized from the south, and more northern regions from the north (Ekman 1922; Markgren 1974; Strandgaard 1982). Recent phylogeographic studies based on mitochondrial DNA (mtDNA) control region sequencing support this colonization scenario (Hundertmark et al. 2002; Niedziałkowska et al. 2014).

Historic records indicate that the Fennoscandian moose population was severely reduced from the 15th century and onwards (Markgren 1974). Intense hunting during the 18th and 19th centuries led to additional dramatic population declines and the species was severely threatened in Norway, Sweden, and Finland in the beginning of the 20th century (Hermansson and Boëthius 1975; Strandgaard 1982). Recovery occurred when commercial forestry in the mid-1900s provided abundant habitat for moose (Markgren 1974). Current population sizes are estimated to be ca. 100,000 in each of Norway and Finland and ca. 300,000 in Sweden (Solberg et al. 2006; Åkesson 2009; Nygrén 2009).

The history of dramatic population reduction may have led to reduced genetic variation. Genetic signatures of a bottleneck in moose have been reported in 1 sample from southern Sweden (Charlier et al. 2008), and low variation at major histocompatibility complex loci in Swedish moose has been suggested to reflect a bottleneck (Ellegren et al. 1996; Mikko and Andersson 1996). However, recent population genetic studies of Norwegian and Finnish moose report no genetic evidence of population reductions (Haanes et al. 2011; Kangas et al. 2013).

Early allozyme studies indicated that although moose are highly mobile, there is substantial spatial differentiation and distinct allele frequency heterogeneities even over short geographic distances (Ryman et al. 1977, 1980; Reuterwall 1980, 1981; Chesser et al. 1982). Among a total of ca. 20 sampling sites distributed all over Fennoscandia, 5 polymorphic allozyme loci detected low levels of genetic variation (Reuterwall 1980) and 5 main genetic groups (Ryman et al. 1980). Recent extensive studies of moose genetic structure in Norway (Haanes et al. 2011) and Finland (Kangas et al. 2013) detected between 2 and 3 genetic groups in Norway, and the authors suggested that the genetic patterns reflect 1) an ancient division into a northern and a southern cluster, and 2) a more recent central population (Haanes et al. 2011). In Finland, 2 subpopulations were reported—a northern and a southern one—and these were concluded to be of relatively recent origin (Kangas et al. 2013).

The objective of the present paper is to quantify genetic variation at multiple spatial scales in moose in Sweden and to relate these patterns to regional genetic structure and evolutionary history, and to the practical management of this heavily harvested animal. We used an existing tissue bank of over 20,000 moose sampled throughout Sweden over 30 years ago with geographical coordinates for each animal, and allozyme genotypes at 3 loci. We combined these data with new genotypic information at microsatellite and mtDNA markers for subsets of the samples to address the following questions: 1) What is the contemporary population structure of moose in Sweden? 2) How many historic lineages are present? 3) Is there genetic evidence of bottlenecks and are they temporally coincident with documented demographic changes in the population? 4) What are the conservation genetic and management implications of the observed genetic structure?

Materials and Methods

Samples and data

We make use of an extensive data set comprising over 20,000 georeferenced frozen moose tissue samples collected over 30 years ago throughout Sweden and genotyped at 3 allozyme loci. The samples are kept at a frozen tissue bank collection maintained by 2 of the authors (LL, NR) at Stockholm University. The data set that we present here consists of 20,358 moose taken in the hunt of 1980. These data have not been analyzed jointly or published previously although separate parts of the collection have been presented in earlier studies, and genotyping methods for scoring the allozyme loci (*Pmi*, *Mdh-2*, *Pgi-1*) are given in those studies (Ryman et al. 1977, 1980; Reuterwall 1980, 1981; Chesser et al. 1982). Information on geographic site of samples, statistical analyses, and basic summary statistics for those loci are presented in Supporting Information S1.

A subsample of 1,207 of the 20,358 moose was genotyped at 12 microsatellite loci, and these individuals were selected to create an even spatial distribution of samples (Fig. 1a; Supporting Information S1). The vast majority of the genotyping was contracted to the Center of Evolutionary Applications, University of Turku, Finland, and methods are described in Supporting Information S2. Combining allozyme and microsatellite data provided genotypes at a total of 15 loci (3 allozymes and 12 microsatellites).

In addition, 48 of the 1,207 individuals representing the 2 major subpopulations that we identified (below; $n = 20$ per subpopulation) and the transition zone between them ($n = 4$ from each of the northern and southern parts of the transition zone) were analyzed for mtDNA variability to address the question of evolutionary age of the genetic groups. Sequencing procedures are described in Supporting Information S2. Four of the 48 mtDNA control region sequences were excluded due to heteroplasmy.

mtDNA diversity

Diversity of mtDNA control region sequences was estimated as nucleotide (π) and haplotype (h) diversities in DnaSp v. 5.10 (Librado and Rozas 2009). mtDNA sequences were analyzed to test for departure from mutation-drift equilibrium with Tajima's D (Tajima 1989) based on the frequency of segregating nucleotide sites. Population pairwise linearized F_{ST} values were computed in Arlequin 3.5 by using the Tamura and Nei nucleotide substitution model (Reynolds et al. 1983).

Net pairwise divergence (d_A) was estimated with MEGA v6 (Tamura et al. 2013). Statistical testing of the null hypothesis of genetic homogeneity between genetic clusters was also performed in Arlequin.

Microsatellite and allozyme population genetic analyses

We applied both individual-based techniques and traditional approaches with a priori grouping of samples to examine spatial allele frequency patterns. The data set of 1,207 moose (15 loci) was grouped into genetic clusters as identified from individual-based analyses in Structure and Tess. *F*-statistics for all loci (Weir 1996) and R_{ST} for microsatellites (Slatkin 1995) were calculated for the grouped data to quantify and test for spatial heterogeneity and deviations from Hardy–Weinberg (HW) proportions in Genepop 3.4 (Raymond and Rousset 1995) and FSTAT 2.9.3 (Goudet 1995). Potential differences in levels of genetic variation (expected heterozygosity, number of alleles, and allelic richness) between regions were tested with unweighted paired *t*-tests (Nei 1987:184). We investigated possible indications of scoring problems and null alleles using Micro-checker (van Oosterhout et al. 2004), and potential indications of selection using Lositan (Beaumont and Nichols 1996; Antao et al. 2008).

Individual-based approaches.—The most likely number of populations (clusters; *K*) compatible with observed genotypic distributions without prior spatial information was assessed using Structure 2.3 (Pritchard et al. 2000; Falush et al. 2003). We used the 4 default models of Structure referring to excluding or including assumptions on "admixture of genomes within individuals" and "correlated allele frequencies among populations" (1–4; cf. Pritchard et al. 2007), and estimations of *K* under each model were replicated over 10 runs. For parameter estimates of allele frequencies, *Q* (individual assignment probability to cluster), and likelihood values for different numbers of *K*, both burn-in length and the number of Markov chain Monte Carlo iterations (MCMC) were 500,000. For each *K* value (1–15), average posterior probability among runs and *SE* were calculated. The main genetic structure of the data set was interpreted from ΔK (cf. Evanno et al. 2005). Individual *Q* values were averaged over 10 runs with Clumpp (Jakobsson and Rosenberg 2007). The geographic distribution of genetic clusters was assessed by comparing individuals' *Q* with their geographic sampling locations, identifying subpopulations from areas with consistently high probabilities of assignment to a particular cluster ($Q > 0.8$), and transition zones from areas with intermediate *Q* coefficients indicating a high degree of admixture.

We used the Bayesian clustering algorithm of Tess 2.3 (Chen et al. 2007; Durand et al. 2009) to assess spatial genetic clustering when taking information on geographic location of individual moose into account. The admixture model of Tess was run 50 times for different maximal numbers of genetic clusters (K_{max} = 2–6, after a test run of K_{max} = 2–15) using a linear trend surface, a conditional autoregressive variance of 1.0, a spatial interaction strength of 0.6 for spatial autocorrelation, and 50,000 MCMC iteration sweeps with a burn-in period of 40,000. For each run, the models' predictive ability is calculated as the Deviance Information Criterion (DIC) expressing model fit penalized by model complexity (Spiegelhalter et al. 2002). For each K_{max}, the 10 runs with the lowest DIC values were selected. Genetic structure was interpreted from the effective number of clusters identified by the K_{max} model where the decreasing DIC averages reach a plateau (Durand et al. 2009), and from the delta statistic of Evanno et al. (2005) calculated for DIC. The distribution of subpopulations and admixture were assessed in the same way as with Structure.

Spatial aspects of genetic variation

We used 2 approaches to describe genetic correlation over space: spatial autocorrelation and neighborhood size (NS). Spatial autocorrelation describes how genetic similarity among individuals changes over geographic distance, and the pattern observed reflects the result of past and present genetic exchange over generations. In contrast, NS analysis provides an estimate of the average dispersal distance between parent and offspring and thus is an estimate of "gene flow" from one generation to the next.

Spatial autocorrelation.—We used Moran's *I* coefficient (Sokal and Oden 1978a, 1978b; Cliff and Ord 1981) that describes the "genetic correlation" between all pairs of individuals within a particular geographic distance interval (here linear distance between 2 individuals) to investigate the potential correlation between genetic and geographic distance among individuals. We used both the n = 1,207 microsatellite and the n = 20,358 allozyme data sets for these autocorrelations. For the n = 20,358 allozyme data (*Pgi-1* and *Pmi*), we chose distance intervals of 5 km and a maximum distance of 1,000 km, resulting in 200 interval classes with over 117,000 pairs per class (average = 1,034,990 pairs). *Mdh-2* was almost monomorphic and was excluded from the autocorrelation analyses. We also evaluated other distance intervals (100 m, 1 km, etc.) to check that the general pattern was not dependent on a particular size of distance interval (cf. Wartenberg 1989; Smouse and Peakall 1999). Calculations were performed using "in-house" programs (TurboPascal 7.0—Sokal and Oden 1978a algorithms) that could handle our large numbers of observations. We analyzed parts of our samples using SPAGeDi 1.4 (Hardy and Vekemans 2002) to verify consistency. SPAGeDi was also used for the microsatellite data to perform separate analyses for the total data set and for the major identified subpopulations excluding the transition zone between them. Here, we used 20 distance classes and divided samples to provide similar numbers of pairwise comparisons per class (2,763–36,392 pairs per class). Bootstrapped confidence intervals (*CI*s) were estimated with 1,000 permutations.

Neighborhood size.—Rousset's *a* (Rousset 2000) was used to assess NS and dispersal distance as applied in SPAGeDi 1.4 (Hardy and Vekemans 2002). We performed the analyses both on the total data set and separately on the 2 main subpopulations, excluding the transition zone. With Rousset's *a* coefficient, the NS was approximated by the inverse of the slope of the regression curve, NS ≈ 1/*b*-log, where *b*-log is the slope of

the regression of *a* on the logarithm of the geographic distance. 95% *CI*s were estimated with 10,000 permutations.

Neighborhood size is defined as NS = $4\pi D\sigma^2$, where D is the population density and σ^2 is the averaged squared parent–offspring axial distance (Rousset 2000; Sumner et al. 2001). If dispersal is normally distributed, NS is the number of reproducing individuals in a circle of radius 2σ. For individuals at the center of the circle, 87% of the parents are expected to be found within the circle and 13% of the parents are responsible for longer distance dispersal (Wright 1946). Average dispersal distance can be estimated if D and NS are known, and we proceeded as follows to obtain a measure of D. Census size was estimated from multiplying the number of adult males and females killed during the 1980 hunt (78,352 individuals—Swedish EPA 1982) by a factor of 2.5 to reflect the standing winter population of adults (195,880—Swedish Association for Hunting and Wildlife Management 2008; K. Wallin, University of Gothenburg, pers. comm.). We then assumed ratios of genetically effective population size (N_e) to census size (N) of 0.1, 0.2, 0.5, and 1.0 to represent N_e estimates. These N_es were used to obtain estimates of effective density (D_e) by dividing N_e with the size of the study area (cf. Calderon et al. 2007; McMahon et al. 2012). For the major identified subpopulations, we estimated D_e using the number of adults killed in the 1980 hunt in each region, respectively, following the same procedure as for the total population. We estimated NS and σ with *SE*s using the SPAGeDi default value of X = 20 to identify the geographic distance (20σ) over which the regression is applied (see above).

Demographic inference

Population bottlenecks.—To investigate genetic evidence for known population reductions and/or expansions, we used coalescent-based simulations coupled with approximate Bayesian computation (ABC) as implemented in DIYABC v2.0 (Cornuet et al. 2014). We compared summary statistics from 6 simulated hypothetical scenarios of demographic history to summary statistics of the empirical data. Scenario 1 was a null model that assumed constant population size through time. In scenario 2, we modeled an ancient reduction of population size that persisted until present, and scenario 3 assumed an ancient bottleneck (i.e., a population size reduction timed with the last glaciation followed by population expansion). Scenario 4 represents a recent population decline, and scenario 5 a recent bottleneck timed with known population reductions. Finally, scenario 6 assumed a recent expansion. The terms "ancient" and "recent" refer to 800–3,000 and 1–100 generations before sampling, respectively (Supporting Information S3).

The mean number of alleles, gene diversity, and mean allele size variance across the 12 microsatellite loci were used as empirical summary statistics for the subpopulations separately. We used a stepwise mutation model with a single nucleotide insertion rate, which is considered similar to an intermediate 2-phased model regarded as typical for microsatellites (Peery et al. 2012). The values for the demographic parameter priors and the mutation model priors are shown in Supporting Information S3. One million simulations were run for each model and subpopulation, and the results from these were used to generate posterior distributions for the demographic parameters and Factor 2 statistics. To select the best-supported scenario among the 6 models, we used a reduced data set of 300,000 simulations since attempts to perform model choice with the full 1,000,000 data set resulted in repeated crashes of the DIYABC software. Estimated demographic parameters and their *CI*s did not differ markedly between the results based on 300,000 simulations versus 1,000,000 simulations (cf. Supporting Information S3). The relative posterior probabilities of each of the 6 scenarios were assessed by selection of the 1% simulated data sets closest to the observed data set using the logistic approach following Beaumont (2008). The confidence in scenario choice was evaluated by simulating 500 new pseudo-observed data sets (PODs) generated under the best-supported scenario and by calculating the proportion of instances where the best-supported scenario had the highest posterior probability, corresponding to an estimation of the type I error rate. Finally, we performed a model validation by simulating 1,000 PODs under the selected demographic scenario (cf. Supporting Information S3). In this procedure, we added the mean Garza-Williamson's index as summary statistics and compared the distributions of the PODs values for each simulated statistics to the observed value (Cornuet et al. 2014).

RESULTS

There were no indications of null alleles or selection at any of the 15 autosomal loci included in this study. Complete genotypes at the 12 microsatellite loci were obtained from 948 individuals with a total of 1,092 individuals being scored for at least 10 loci. Summary statistics for the combined microsatellite and allozyme data set divided on the basis of the 2 major subpopulations identified and the transition zone between them (Fig. 1b) and the 4 TESS clusters (Fig. 1c) are provided in Table 1. In total, 97 alleles were observed (91 microsatellite and 6 allozyme) resulting in an average allelic richness between 4.21 and 5.48 and average expected heterozygosities between 0.47 and 0.55.

Population structure.—All analyses indicate that the Swedish moose population is strongly substructured. The distribution of allele frequencies among 50×50 km squares for the 20,358 individual moose data reveals a complex allelic landscape with sharp allele frequency shifts at both *Pgi-1* and *Pmi* allozyme loci (Fig. 2; *Mdh-2* is only weakly polymorphic; Supporting Information S1). STRUCTURE analyses of our multilocus data set (allozymes + microsatellites) provided highly consistent results indicating $K = 2$ as the most likely scenario. The likelihood values level off at $K = 2$, and we observe the highest ΔK for $K = 2$. The 2 major clusters are geographically separated into northern and southern regions with a transition zone that consists of individuals with predominantly intermediate assignment probabilities (Fig. 3; Supporting Information S4). The proportion of individuals with an admixed genome (defined as assignment probabilities, Q, in the range 0.2–0.8) are 0.08 and 0.07 in the northern and southern subpopulations, respectively, and 0.37

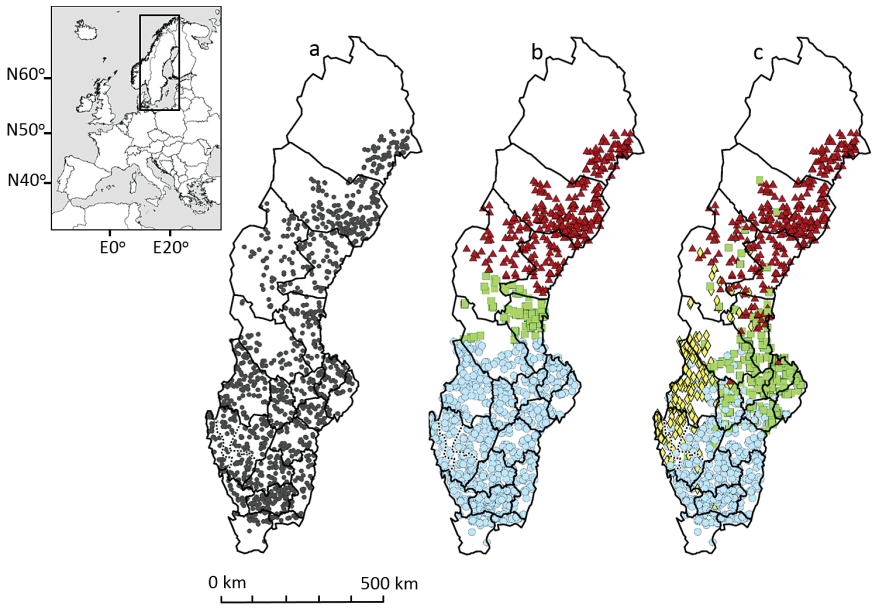

Fig. 1.—Distribution of 1,207 moose taken from throughout Sweden and genotyped at 12 microsatellite loci (out of 20,358 scored for 3 allozyme loci; Supporting Information S1), each mark representing 1 moose. a) Sample distribution. b) The 2 major subpopulations predominantly containing individuals strongly assigned to a northern or southern genetic cluster (cf. Fig. 3). Green squares represent individuals in a transition zone with predominantly admixed assignment values in the STRUCTURE analysis. c) Four genetic clusters identified with the software TESS (that takes both genotype and geographic location of samples into account) and assigning each individual to a genetic cluster based on highest assignment probability. Solid lines indicate current Swedish county borders, whereas dotted lines show additional county borders that existed in 1980 when the samples were collected (cf. Supporting Information S1).

Table 1.—Statistics for subpopulations identified by the softwares STRUCTURE (Pritchard et al. 2000) and TESS (Chen et al. 2007; cf. Figs. 1b and 1c). The transition zone between the STRUCTURE subpopulations is treated as a separate group and the total is based on estimates on all 3 groups. H_o and H_e = observed and expected heterozygosity. R_{ST} is based only on microsatellite data. Mean allelic richness for the total data set is lower for the STRUCTURE populations than for the TESS populations because rarefaction is based on the smallest sample size (n = 86 in the transition zone). *P < 0.05, ***P < 0.001.

Subpopulation	n	Mean allelic richness/locus	Mean number of alleles/locus	Number of private alleles	H_e	H_o	F_{IS}	F_{IT}	F_{ST}	R_{ST}
STRUCTURE (Fig. 1b)										
North	333	4.934	5.667	12	0.526	0.506	0.020*			
South	788	4.217	5.400	9	0.518	0.540	0.060***			
Transition zone	86	4.751	4.800	0	0.551	0.483	0.005			
Total	1,207	4.890	6.467		0.541	0.493	0.045***	0.132***	0.092	0.067
TESS (Fig. 1c)										
North	366	5.480	5.800	11	0.518	0.507	0.029*			
South-east	212	4.991	5.067	1	0.474	0.468	0.028*			
South-west	187	5.112	5.133	3	0.560	0.551	0.023			
South-south	442	4.348	4.800	3	0.489	0.469	0.040***			
Total	1,207	5.319	6.467		0.541	0.493	0.032***	0.109***	0.081	0.057

in the transition zone. Average Q values to the northern cluster were 0.93, 0.52, and 0.06 for individuals sampled in the northern, transition, and southern groups, respectively.

When information on geographic location is included in the clustering analysis using the TESS algorithm, the most likely structuring is 4 groups as indicated by a plateau in decreasing DIC averages and the highest ΔDIC at K_{max} = 4 (Supporting Information S5). The geographic location of the northern cluster suggested by TESS coincides with the northern subpopulation identified by STRUCTURE (Figs. 1b and 1c), and the assignment probabilities to the northern cluster in STRUCTURE and TESS are strongly correlated (r = 0.94, $F_{1,1205}$ = 8,761, P < 0.001). The 3 additional clusters proposed by TESS divide the southern subpopulation of STRUCTURE into 3 regions—a south-eastern, a south-western, and a south-southern one (Figs. 1b and 1c). We also performed iterative STRUCTURE analyses where the northern and southern clusters were run separately, and these analyses indicate K = 1 and K = 3 as the most likely number of clusters for the northern and the southern groups, respectively, in agreement with the TESS results (details not shown).

Levels of genetic variation and HW proportions of identified groups.—The levels of genetic variation and F_{IS} values of the

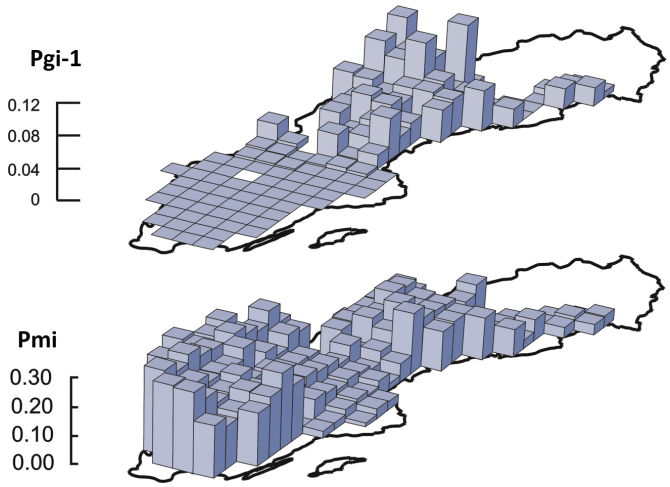

Fig. 2.—Frequency of the less common allele at the *Pgi-1* and *Pmi* allozyme loci in 50 × 50 km squares covering Sweden (n = 20,358). The allele frequency at *Pgi-1* is zero (0) in the southern part of Sweden.

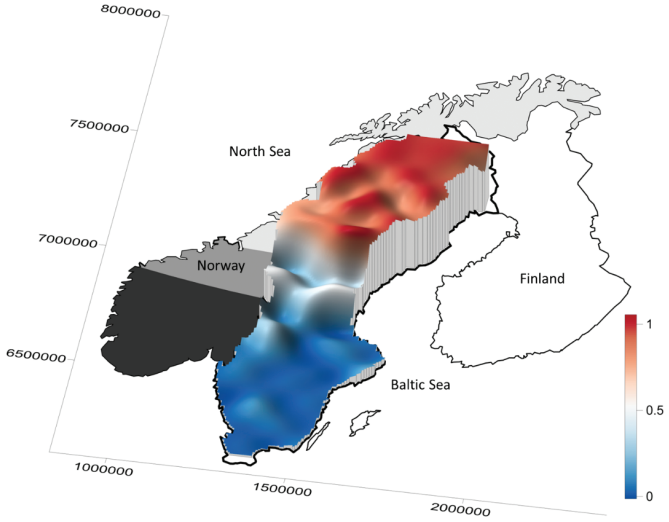

Fig. 3.—Color coded 3D surface plot of assignment probabilities to the northern (red) of the 2 major clusters identified by the software Structure (Pritchard et al. 2000) based on 1,207 moose samples collected throughout Sweden (cf. Fig. 1a) and genotyped at 15 loci (12 microsatellites and 3 allozymes). Red indicates strong assignment to the northern cluster, while blue signifies high assignment to the southern one. There is a transition zone in central Sweden with individuals of predominantly intermediate assignment probabilities to both clusters (white-gray color code). The 2 major clusters previously identified in Norway by Haanes et al. (2011) are also shown: a southern Norwegian cluster (dark shade), a northern one (light shade), and a transition zone between them (medium shade). Geographic coordinates on the axes are given in SWEREF99TM (cf. Supporting Information S4).

northern and the southern main subpopulations, the transition zone between them, and the substructures detected with Tess are summarized in Table 1. Deviations from HW proportions in the southern main subpopulation indicate further structuring, and when considering the 3 Tess clusters of the south (south-eastern, south-western, and south-southern), deficiencies of heterozygotes are somewhat reduced.

Levels of variation are somewhat higher in the north than in the south in terms of expected heterozygosity (H_e), number of alleles, as well as allelic richness (Table 1). These differences are not statistically significant for heterozygosity or number of alleles, but there is significantly higher allelic richness in the north than in the south (t_{14} = 3.55, P < 0.01). H_e is higher in the transition zone than in the other 2 regions, but this difference is not statistically significant. Allelic richness is, however, significantly higher in the transition zone than in the south (t_{14} = 2.51, P = 0.02).

Genetic divergence between identified groups.—F_{ST} between the northern and southern subpopulation is 0.10 for the microsatellite loci (0.09 when including allozymes; Supporting Information S1). R_{ST} values are lower than F_{ST} at most loci, although this difference is not significant (paired t-test, t_{11} = 1.95, P = 0.08); overall R_{ST} = 0.07. Pairwise F_{ST} between the 4 groups identified by Tess range between 0.04 and 0.13 (including all 15 loci) with the largest value observed between the northern and the south-southern subpopulation.

mtDNA control region sequencing.—The 44 mtDNA control region sequences were analyzed for 568–643 nucleotides, and we found a total of 7 haplotypes (Table 2). One single haplotype (number 2 in our study, see Supporting Information S6) comprised 80% of the samples and was spread evenly throughout Sweden, consistent with previous studies (Hundertmark et al. 2002; Niedziałkowska et al. 2014). We observed no significant mtDNA differentiation between the north and the south (net pairwise divergence, $d_A \approx 0.00\%$, F_{ST} = 0.087, P = 0.078), so there is no evidence of the northern and southern clusters representing different ancestral lineages. The southern population shows higher mtDNA variation than the northern one measured both as haplotype diversity (h = 0.42 versus 0.23) and nucleotide diversity (π = 0.0041 versus 0.0025; Table 2). A statistically significant negative Tajima's D was observed for the northern subpopulation (Table 2); this is usually interpreted to indicate a population size expansion and/or purifying selection (Tajima 1989). See Supporting Information S6 for further results from our mtDNA analyses.

Table 2.—Summary statistics of genetic variability at the mitochondrial control region for the northern and southern cluster and the transition zone (cf. Supporting Information S4). Values include the total number of sequences analyzed (*N*), sequence length in base pairs (bp), number of segregating sites (*S*), number of haplotypes (*Nh*), number of private haplotypes (PrHap), which of the 7 haplotypes that occurred in each cluster (Hap; Supporting Information S6), haplotype diversity (*h*), variance of haplotype diversity (*V*(*h*)), nucleotide diversity (π), and Tajima's *D*. ** = tail-area probability < 0.01.

Cluster	*N*	bp	*S*	*Nh*	PrHap	Hap	*h*	*V*(*h*)	π (%)	Tajima's *D*
Northern	17	568	11	3	2	1, 2, 6	0.23	0.017	0.25	−2.12**
Transition zone—north	4	568	1	2	1	2, 5	0.50	0.070	0.09	−0.61
Transition zone—south	3	568/643	0	1	1	2, 7[a]	0	0.000	0.00	0.00
Southern	20	568	6	3	2	2, 3, 4	0.42	0.013	0.41	1.17
Overall	44	568/643	15	7	6	1–7	0.33	0.079	0.31	−1.55

[a]Haplotype 7 that includes an extra 75 bp insertion has not been included in the diversity estimates.

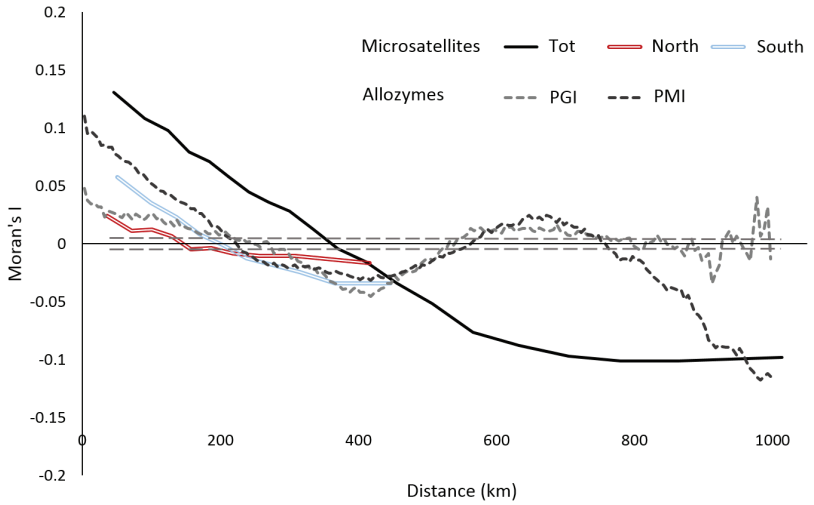

Fig. 4.—Spatial autocorrelograms (Moran's *I*) for 12 microsatellites in 1,207 individual moose in Sweden and for 2 allozymes (*Pgi-1* and *Pmi*) in 20,358 moose. Allozyme distance classes are consistently 5 km, whereas microsatellite distance classes were constructed to provide equal numbers of pairs per class. A 95% *CI* for expected values under random spatial distribution for 1,207 individuals and 12 microsatellite loci are indicated with dotted lines in the figure (close to the line indicating Moran's $I = 0$).

Spatial autocorrelation analyses.—The autocorrelation results are presented graphically in correlograms depicting how the genetic correlation between individuals, measured as Moran's *I*, changes with increasing geographic distance (Fig. 4). *Pgi-1* and *Pmi* of the 20,358 moose data show pronounced structuring (Fig. 4). *Pgi-1* is only variable in the central and northern parts of Sweden, and only these regions were included in the correlogram for this locus. For both loci, the correlogram intercepts the x-axis at just over 200 km, and Moran's *I* decreases almost linearly within distances of 200 km at both loci (a so-called continuous cline). The statistical interpretation of the x-intercept is that below this distance moose are (on average) genetically more similar than 2 randomly selected ones from the total collection, and this distance is sometimes referred to as "genetic patch size" (Sokal and Wartenberg 1983; Diniz-Filho and Telles 2002).

For the microsatellite data set (n = 1,207), the correlogram intercepts at about 370 km for the total data set corresponding to an almost doubled genetic patch size as compared to the allozyme (n = 20,358) data (intercepts at 370 versus 250 km). Within each of the northern and southern subpopulations, the intercepts are about 150 and 210 km, respectively (Fig. 4). We also performed the autocorrelation analyses on each sex separately, which resulted in correlograms almost identical to those for both sexes combined (not shown). There are no major intercept differences between the 4 TESS clusters, i.e., when the southern subpopulation is further divided into 3 smaller clusters. X-axis intercepts for those 4 TESS clusters are: northern: c. 180 km, south-eastern: c. 130 km, south-western: c. 140 km, and south-southern: c. 150 km.

NS and dispersal distance.—We estimated the population density to be 0.51, 1.32, and 0.81 individuals/km^2 for the northern, southern, and the total population, respectively. Effective population densities used for estimation of average dispersal distances (σ) were thus 0.1, 0.2, 0.5, and 1.0 of these values, respectively (based on our assumptions of N_e/N ratios).

Rousset's *a* increased with spatial distance within each of the northern and the southern clusters and for the total population ($P < 0.001$ in all cases), allowing estimation of NS and the corresponding genetic dispersal distances (Hardy and Vekemans 2002). NS estimates under different N_e/N assumptions were NS = 80–145 for the northern cluster, 76–201 for the southern cluster, and 61–164 for the total population. The lowest estimates of NS correspond to the $N_e/N = 0.1$ assumption, and the highest ones for $N_e = N$. Solving $NS = 4\pi D_e \sigma^2$ for the mean axial parent–offspring distance (σ^2) yields an estimated dispersal distance (σ) of 4.75–11.11 km in the northern subpopulation, 3.45–6.75 km in the southern one, and 4.00–7.77

km for the total data set. The lowest estimate of σ corresponds to a $N_e/N = 1$. Details on NS and σ estimates can be found in Supporting Information S7.

Bottlenecks.—We find genetic support for bottlenecks both in the northern and southern subpopulations. For both groups, the highest posterior probability was observed for scenario 5 (Table 3; Supporting Information S3), which assumes a recent bottleneck with a severe reduction in the effective population size followed by a re-expansion. This scenario was selected with high posterior probabilities (north: 70.5%, *CI* 69.3–71.6%; south: 58.4%, *CI* 57.1–59.7%), whereas the other 5 scenarios had lower probabilities (Table 3). Using the subroutine for "Confidence in scenario choice analysis" implemented in DIYABC, the statistical power to select the right scenario was high in both the northern and southern subpopulations (67% and 63%, respectively). For both populations, analyses of scenario 1 (constant population size) provided very low support, with less than 1% posterior probabilities.

When posterior distributions were recovered for scenario 5, using the best fitting 1% of the 1,000,000 simulated data sets, we found that effective population sizes in both subpopulations appear to have been reduced to a few percentages of their former size. In both cases, the estimated bottlenecks were long and relatively recent, lasting for a hundred generations or more, and ending only a few up to less than a hundred generations before sampling (based on the mode values; Table 4). In the south, we estimated a reduction of effective population size to 1.7% of the former size: from N_e = 24,900 (90% HDPI: 10,300–203,000) to N_e = 414 (90% HDPI: 152–806) based on the mode value of the marginal posterior probability density. In the north, the effective population size during the bottleneck was estimated as 2.7% of the pre-decline size: from N_e = 12,900 (90% HDPI: 12,200–237,000) to N_e = 350 (90% HDPI: 175–2,230).

The ABC analyses suggest that the populations recovered after the bottlenecks (Table 4). Moreover, the estimated timing of the bottlenecks fits known population reductions well. We estimated the bottleneck in the southern subpopulation to have ended around 4 generations before sampling (90% HDPI: 2.3–65.4). Assuming a generation time of 7 years (Gaillard 2007), this suggests that the bottleneck ended around 1950. For the northern population, the end of the bottleneck was estimated as 20 generations before sampling (90% HDPI: 8.5–92.7), i.e., around 1840.

Table 3.—Relative posterior probabilities of the 6 demographic scenarios (cf. Supporting Information S3) for the northern and the southern subpopulation, respectively, using a logistic regression on the 1% simulated data sets closest to the observed values. The subpopulations were defined as in Fig. 1b, excluding the transition zone.

Scenario	Posterior probability (%)	95% *CI* lower–upper (%)
South		
Sc1	0.14	0.00–0.93
Sc2	36.53	35.17–37.89
Sc3	4.64	3.79–5.49
Sc4	0.23	0.00–1.02
Sc5	58.40	57.07–59.73
Sc6	0.06	0.00–0.84
North		
Sc1	1.73	1.35–2.11
Sc2	12.27	11.49–13.05
Sc3	12.57	11.74–13.40
Sc4	0.13	0.00–0.32
Sc5	70.46	69.33–71.60
Sc6	2.84	2.36–3.33

DISCUSSION

Our results show that moose exhibit genetic structuring over Sweden that is characterized by isolation by distance in combination with occasional sharp allele frequency shifts. We find a minimum of 2 major subpopulations, a northern and a southern one, with a transition zone between them featuring low assignment probabilities to both of the 2 main clusters, sharp genetic changes, and tendencies for elevated levels of genetic variation. These major genetic groups coincide with similar subdivisions in Norway (Haanes et al. 2011). The Norwegian samples were collected over 30 years later than the samples in our study, suggesting that the structure we detect has remained stable at least over the past few decades. There is also a fine-scale substructuring within the southern subpopulation that includes 3 subclusters—a south-western, a south-eastern, and a south-southern. In contrast, such distinct and geographically separated subclusters were not detected in the north.

Levels of genetic variation and spatial structuring.—Genetic variation of the microsatellites is similar to that observed in other studies of moose in Scandinavia (Charlier et al. 2008; Haanes et al. 2011) although heterozygosity is somewhat lower than in Finland (Kangas et al. 2013). Allelic richness is significantly higher in the northern subpopulation than in the southern one, similar to what has been reported for the Norwegian moose population (Haanes et al. 2011). We find higher observed and expected heterozygosities in the transition zone, and although these differences are not statistically significant, they suggest admixture between 2 differentiated populations (Table 1). The mtDNA data show a somewhat contrasting pattern with respect to levels of variation since haplotype and nucleotide diversities are both higher in the south than in the north (Table 2).

The large number of individuals genotyped for the 3 allozyme loci enabled detailed illustration of allele frequency shifts over Sweden. The pattern of pronounced allele frequency change of *Pgi-1* in central Sweden is remarkably similar to the genetically neutral multilocus signal of subdivision of the Swedish moose population into 2 major subpopulations, but not a driver of these patterns. The identification of genetic clusters by the softwares STRUCTURE and TESS was the same regardless of whether *Pgi-1* was included or not. Our present results in combination with the observations from Norway (Haanes et al. 2011) and Finland (Kangas et al. 2013) are in line with what was observed already in an early allozyme study, a subdivision of the Fennoscandian moose population into at least 5 subgroups, including a divergence between northern and southern Sweden (Ryman et al. 1980).

Table 4.—Effective population size (N_e) estimates from ABC analyses under the best-supported scenario (scenario 5; Supporting Information S3) of a recent bottleneck in the southern and northern subpopulations (Fig. 1b, excluding the transition zone). The median, mode, 90% highest density probability interval (HDPI), and Factor 2 for the median are given for each parameter. ABC = approximate Bayesian computation; SNI = single nucleotide insertion rate.

Estimated parameter	Median	Mode	90% HDPI	Factor 2 (median)
South				
N_e before bottleneck	56,700	24,900	10,300–203,000	0.772
N_e during bottleneck	442	414	152–806	0.894
N_e after bottleneck	103,000	7,280	7,870–231,000	0.736
Length of bottleneck (generations)	345	491	98.9–488	0.788
End of bottleneck (number of generations before sampling)	12.8	4.1	2.3–65.4	0.710
Mutation rate$_{mic}$	2.19×10^{-4}	1.18×10^{-4}	1.06×10^{-4}–7.52×10^{-4}	0.792
SNI$_{mic}$	1.93×10^{-7}	1.47×10^{-8}	1.28×10^{-8}–5.33×10^{-6}	0.436
North				
N_e before bottleneck	24,700	12,900	5,740–101,000	0.786
N_e during bottleneck	597	350	175–2,230	0.852
N_e after bottleneck	123,000	32,700	12,200–237,000	0.750
Length of bottleneck (generations)	332	493	78.6–486	0.786
End of bottleneck (number of generations before sampling)	45.8	20.1	8.5–92.7	0.718
Mutation rate$_{mic}$	2.72×10^{-4}	1.19×10^{-4}	1.16×10^{-4}–8.03×10^{-4}	0.834
SNI$_{mic}$	2.58×10^{-7}	1.33×10^{-8}	1.35×10^{-8}–6.10×10^{-6}	0.336

Our study confirms the presence of several mtDNA haplotypes in Sweden, but we found no significant genetic divergence between northern and southern Sweden. It should be noted, however, that the estimated genetic differentiation is relatively large (F_{ST} = 0.09) and nearly significant (P = 0.08), despite being based on a fairly small number of individuals (n = 17 and 20). Two haplotypes have previously been described in Swedish moose (Hundertmark et al. 2002; Niedziałkowska et al. 2014); we find both in our study. In addition, we find a haplotype in northern Sweden that previously had only been found in moose in Finland (Niedziałkowska et al. 2014). Four of our haplotypes have not previously been reported (Supporting Information S6).

Dispersal distance and genetic divergence over space.—Our analyses of NS indicate that most dispersal is relatively restricted over space in spite of moose being highly mobile animals with potential for long-distance migration. For instance, the average dispersal distance is only a few kilometers (σ = 3.5–11.1 km), in line with earlier results from radiotracking providing home range estimates of 10–30 km^2 (Cederlund et al. 1987; Sweanor and Sandegren 1988, 1989; Cederlund and Sand 1992). This restricted dispersal distance indicates that gene flow from one generation to the next occurs, on average, over short distances. Over multiple generations, the genetic exchange expands over space, however; all correlograms show fairly steep slopes that do not level off until the largest distances. This suggests a more or less continuous genetic change where divergence within the major clusters increases uniformly with geographic distance.

The biological interpretation of genetic patch size (correlogram x-axis intercept) in situations of continuous clines is insufficiently dealt with in the literature, and we suggest that such estimates should be implemented with caution. When sampling from a continuous cline, the genetic patch size, which represents the maximum distance at which 2 individuals are more related than 2 random individuals from the sample, is expected to increase as geographic sampling area grows. We propose that in such cases the genetic patch size should correspond to half the maximum geographic distance and increase as the area under study grows. Preliminary analytical results and computer simulations support this contention, in line with the observation that estimated patch size within the northern and southern subpopulations is about half of that for the total sample (Fig. 4).

In our separate analysis of allozyme loci, the smaller half of the distance classes in the autocorrelograms coincide well with those for the northern and southern subpopulations based on microsatellites, again supporting restricted gene flow over space resulting in a continuous genetic change. At large distances, the allozyme correlograms intercept the x-axis more than once, reflecting similar allele frequencies between geographically distant areas (Fig. 2); this similarity only refers to an allele at a single locus, though, and should not be interpreted as a general genetic pattern over multiple loci. The restricted gene flow over Sweden indicated by our results is in line with previous genetic studies (Ryman et al. 1977, 1980; Reuterwall 1981; Chesser et al. 1982; Charlier et al. 2008).

Bottlenecks and evolutionary history of moose in Fennoscandia.—It is known that the Swedish moose population was severely reduced due to intense hunting from the 18th century onwards resulting in the species being threatened by the early 20th century. Populations in Norway and Finland experienced similar declines (Hermansson and Boëthius 1975; Strandgaard 1982). Our ABC analysis detected genetic evidence of these known demographic changes. The most likely simulated scenario suggested recent bottlenecks with subsequent population expansion in both the southern and the northern subpopulation. The estimated timing of these bottlenecks fits the known population reduction well, even though it should be noted that the *CI*s are very large and span from medieval times to the 1950s. The estimated lengths of the bottlenecks are hundreds of generations with the posterior distributions

approaching the maximum prior (set to 500 generations). In combination with fairly high support for scenario 2 in the ABC analysis (ancient reduction), this leads us to believe that the demographic history of moose in Sweden is likely to be more complicated than a single population reduction during the period spanning the 18–20th century. This is in line with historic records indicating population reductions already during the 15th century (Markgren 1974).

There are no indications that the divergence time since the split between the northern and the southern subpopulation is ancient, rather we suggest that the division into 2 major subpopulations of moose in Sweden is of relatively recent origin, occurring after postglacial colonization. First, the R_{ST} values between north and south are not larger than the F_{ST} values. Thus, differences in allele frequencies between regions do not seem to have been shaped by new mutations, as would have been expected if the divergence was ancient (Slatkin 1995). Second, the same mitochondrial haplotypes are found in the north and the south, suggesting that the same lineage colonized all of Sweden after the last glacial maximum. The current Swedish and Norwegian moose populations thus appear to represent an ancient genetic lineage of moose that colonized Fennoscandia from the south after the last glaciation. The recently published work of Niedziałkowska et al. (2014) supports this contention—those authors find that moose in Norway and Sweden are characterized by a western mtDNA clade that is rare in other parts of Europe. Those authors also suggest that Finnish moose originate, at least in part, from a separate glacial refugium as has also been suggested previously (Markgren 1974; Hundertmark et al. 2002).

Divergence time between subpopulations reported in previous studies in Scandinavia was estimated as ~ 800–1,500 generations ago in Norway, corresponding to ~ 6,000–10,000 years (Haanes et al. 2011), versus 96–238 years in Finland (Kangas et al. 2013), and both studies used ABC approaches. In our study, we first tried to estimate the timing of split between the 2 major subpopulations without success/support (data not shown). This could be due to a more complex demographic history than the scenarios we have been able to simulate. Such a complex history might be a reason for the large difference in estimated divergence time between subpopulations reported for Finland (Kangas et al. 2013) versus Norway (Haanes et al. 2011).

Conservation and management implications.—The moose has a long history of being controlled and hunted by humans in Sweden as well as in the rest of Fennoscandia, and harvest has the potential to cause 3 main types of genetic change; 1) alteration of population subdivision, 2) loss of genetic variation, and 3) selective genetic changes (Laikre and Ryman 1996; Allendorf et al. 2008).

Today, we see no immediate risks of loss of genetic variation from type 1) and 2) effects because the current moose population is very large and subpopulations occur over large areas. Moose management in Sweden occurs at the county level where each county is divided into moose management areas, and hunting pressure is determined on the basis of estimates of the number of animals within such areas. The major genetic subpopulations identified in this study, and the transition zone between them, extend over several counties (Figs. 1b and 1c). This indicates a good potential for avoiding overhunting of an entire genetic subunit.

However, we found that it is possible that harvest of the Swedish moose population historically has had effects on genetic variation. We found indications of past genetic bottlenecks in our data that appear to coincide with strong demographic reductions caused or enhanced by human actions (Markgren 1974; Strandgaard 1982). The split of the Swedish moose into 2 subpopulations has most likely occurred after postglacial recolonization of Scandinavia and can be the result of depleted population sizes causing genetic drift within small populations, leading to allele frequency differences between post-bottleneck populations. The fact that the substructures remain today could be an effect of human-induced pressures if, e.g., strong hunting reduces gene flow as has been suggested for brown bear in Finland (Hagen et al. 2015). It is also possible that current population genetic structure, although influenced by bottlenecks, represents pre-bottleneck genetic differentiation as has recently been shown for brown bear in Sweden (Xenikoudakis et al. 2015).

Based on currently available information, we recommend that the genetic structure of moose is considered and monitored to safeguard the continued existence of the variation represented by genetically divergent groups. Further, it is important that the current Swedish and Norwegian moose population as a whole is maintained as it appears to represent the only remainder of an ancient lineage of moose that colonized Fennoscandia from the south after the last glaciation (Niedziałkowska et al. 2014). Demographic reductions of separate subpopulations of this genetic cluster will result in loss of genetic variation and overlooking genetic resources on a regional scale might lead to unintended consequences.

Acknowledgments

We thank R. Ogden, C. Wheat, G. Gamberale Stille, and 4 anonymous reviewers for valuable comments, and R. Salamon for assistance. Grants and financial support from the Swedish Research Council Formas (LL), the Swedish Research Council VR (NR, LD), the Swedish Environmental Protection Agency (LL), and the Carl Tryggers Foundation (LL) are gratefully acknowledged.

Supporting Information

The Supporting Information documents are linked to this manuscript and are available at Journal of Mammalogy online (jmammal.oxfordjournals.org). The materials consist of data provided by the author that are published to benefit the reader. The posted materials are not copyedited. The contents of all supporting data are the sole responsibility of the authors. Questions or messages regarding errors should be addressed to the author.

Supporting Information S1.—Samples and allozyme data incl. statistical power and summary statistics.
Supporting Information S2.—Microsatellite genotyping and mtDNA sequencing.
Supporting Information S3.—DIYABC scenarios and settings.
Supporting Information S4.—STRUCTURE analysis and distribution of assignment probabilities.
Supporting Information S5.—TESS summary results for the admixture model.
Supporting Information S6.—mtDNA haplotypes.
Supporting Information S7.—Neighborhood size and dispersal distance.

LITERATURE CITED

ÅKESSON, C. (ed.). 2009. Facts on wildlife and fish. Recent research on wildlife, fish, and management. Information from the Department of Wildlife, Fish and Environmental Studies. Fact sheet No. 4/2009. Swedish University of Agricultural Sciences, Umeå, Sweden (in Swedish).

ALLENDORF, F. W., P. R. ENGLAND, G. LUIKART, P. A. RITCHIE, AND N. RYMAN. 2008. Genetic effects of harvest on wild animal populations. Tree 23:327–337.

ANTAO, T., A. LOPES, R. J. LOPES, A. BEJA-PEREIRA, AND G. LUIKART. 2008. LOSITAN: a workbench to detect molecular adaptation based on a FST outlier-method. BMC Bioinformatics 9:212.

BEAUMONT, M. A. 2008. Joint determination of topology, divergence time, and immigration in population trees. Pp. 134–154 in Simulation, genetics, and human prehistory (S. Matsumura, P. Forster, and C. Renfrew, eds.). McDonald Institute Press, University of Cambridge, United Kingdom.

BEAUMONT, M. A., AND R. A. NICHOLS. 1996. Evaluating loci for use in the genetic analysis of population structure. Proceedings of the Royal Society of London, B. Biological Sciences 263:1619–1626.

CALDERON, I., N. ORTEGA, S. DURAN, M. BECERRO, M. PASCUAL, AND X. TURON. 2007. Finding the relevant scale: clonality and genetic structure in a marine invertebrate (Crambe crambe. Porifera). Molecular Ecology 16:1799–1810.

CEDERLUND, G., AND H. SAND. 1992. Dispersal of subadult moose (*Alces alces*) in a nonmigratory population. Canadian Journal of Zoology 70:1309–1314.

CEDERLUND, G., F. SANDEGREN, AND K. LARSSON. 1987. Summer movements of female moose and dispersal of their offspring. Journal of Wildlife Management 51:342–352.

CHARLIER, J., L. LAIKRE, AND N. RYMAN. 2008. Genetic structure and evidence of a local bottleneck in moose in Sweden. Journal of Wildlife Management 72:411–415.

CHEN, C., E. DURAND, F. FORBES, AND O. FRANCOIS. 2007. Bayesian clustering algorithms ascertaining spatial population structure: a new computer program and a comparison study. Molecular Ecology Notes 7:411–415.

CHESSER, R. K., C. REUTERWALL, AND N. RYMAN. 1982. Genetic differentiation of Scandinavian moose *Alces alces* populations over short geographical distances. Oikos 39:125–130.

CLIFF, A. D., AND J. K. ORD. 1981. Spatial processes: models and applications. Pion Ltd, London, United Kingdom.

CORNUET, J. M., ET AL. 2014. DIYABC v2.0: a software to make approximate Bayesian computation inferences about population history using single nucleotide polymorphism, DNA sequence and microsatellite data. Bioinformatics 30:1187–1189.

DINIZ-FILHO, J. A. F., AND M. P. C. TELLES. 2002. Spatial autocorrelation analysis and the identification of operational units for conservation in continuous populations. Conservation Biology 16:924–935.

DURAND, E., F. JAY, O. E. GAGGIOTTI, AND O. FRANCOIS. (2009). Spatial inference of admixture proportions and secondary contact zones. Molecular Biology and Evolution 26:1963–1973.

EKMAN, S. 1922. Djurvärldens utbredningshistoria på Skandinaviska halvön (Distribution history of the animal world on the Scandinavian peninsula). Albert Bonnier Publishing, Stockholm, Sweden (in Swedish).

ELLEGREN, H., S. MIKKO, K. WALLIN, AND L. ANDERSSON. 1996. Limited polymorphism at major histocompatibility complex (MHC) loci in the Swedish moose *A. alces*. Molecular Ecology 5:3–9.

EVANNO, G., S. REGNAUT, AND J. GOUDET. 2005. Detecting the number of clusters of individuals using the software STRUCTURE: a simulation study. Molecular Ecology 14:2611–2620.

FALUSH, D., M. STEPHENS, AND J. K. PRITCHARD. 2003. Inference of population structure using multilocus genotype data: linked loci and correlated allele frequencies. Genetics 164: 1567–1587.

GAILLARD, J. M. 2007. Are moose only a large deer?: some life history considerations. Alces 43:1–11.

GOUDET, J. 1995. FSTAT (vers 1.2): a computer program to calculate F-statistics. Journal of Heredity 86:485–486.

HAANES, H., K. H. RØED, E. J. SOLBERG, I. HERFINDAL, AND B. E. SÆTHER. 2011. Genetic discontinuities in a continuously distributed and highly mobile ungulate, the Norwegian moose. Conservation Genetics 12:1131–1143.

HAGEN, S. B., A. KOPATZ, J. ASPI, I. KOJOLA, AND H. G. EIKEN. 2015. Evidence of rapid change in genetic structure and diversity during range expansion in a recovering large terrestrial carnivore. Proceedings of the Royal Society of London, B. Biological Sciences 282:20150092.

HARDY, O. J., AND X. VEKEMANS. 2002. SPAGeDi: a versatile computer program to analyse spatial genetic structure at the individual or population levels. Molecular Ecology Notes 2:618–620.

HEWITT, G. M. 2011. Quarternary phylogeography: the roots of hybrid zones. Genetica 139:617–638.

HERMANSSON, N., AND J. BOËTHIUS (EDS.). 1975. The moose: industry and environment - hunting and management. A course book from the Swedish Association for Hunting and Wildlife Management. Proporius förlag, Stockholm, Sweden (in Swedish).

HUNDERTMARK, K. J., G. F. SHIELDS, I. G. UDINA, R. T. BOWYER, A. A. DANILKIN, AND C. C. SCHWARTZ. 2002. Mitochondrial phylogeography of moose (*Alces alces*): Late Pleistocene divergence and population expansion. Molecular Phylogenetics and Evolution 22:375–387.

JAKOBSSON, M., AND N. A. ROSENBERG. 2007. CLUMPP: a cluster matching and permutation program for dealing with label switching and multimodality in analysis of population structure. Bioinformatics 23:1801–1806.

KANGAS, V. M., L. KVIST, S. LAAKSONEN, T. NYGRÉN, AND J. ASPI. 2013. Present genetic structure revealed by microsatellites reflects recent history of the Finnish moose (*Alces alces*). European Journal of Wildlife Research 59:613–627.

LAIKRE, L., L. C. LARSSON, A. PALMÉ, J. CHARLIER, M. JOSEFSSON, AND N. RYMAN. 2008. Potentials for monitoring gene level biodiversity: using Sweden as an example. Biodiversity and Conservation 17:893–910.

Laikre, L., and N. Ryman. 1996. Effects on intraspecific biodiversity from harvesting and enhancing natural populations. Ambio 25:504–509.

Librado, P., and J. Rozas. 2009. DnaSP v5: a software for comprehensive analysis of DNA polymorphism data. Bioinformatics 25:1451–1452.

Luoma, A. 2002. Moose hunting in Finland – management of a heavily harvested population. Ph.D. dissertation, Academy of Science, University of Helsinki, Finland.

Markgren, G. 1974. The moose in Fennoscandia. Le Naturaliste Canadien 101:185–194.

McMahon, B., M. P. Johansson, S. B. Piertney, K. Buckley, and J. Höglund. 2012. Genetic variation among endangered Irish red grouse (*Lagopus lagopus hibernicus*) populations: implications for conservation management. Conservation Genetics 13:369–647.

Mikko, S., and L. Andersson. 1996. Low major histocompatibility complex class II diversity in European and North American moose. Proceedings of the National Academy of Science 92:4259–4263.

Nei, M. 1987. Molecular evolutionary genetics. Columbia University Press, New York.

Niedziałkowska, M., et al. 2014. Spatial structure in European moose (*Alces alces*): genetic data reveal a complex population history. Journal of Biogeography 41:2173–2184.

Nygrén, T. 2009. Biology and policies in Finnish moose population regulation and management. Ph.D. dissertation, University of Joensuu, Finland.

Peery, M. Z., et al. 2012. Reliability of genetic bottleneck tests for detecting recent population declines. Molecular Ecology 21:2403–3418.

Pritchard, V. L., K. Jones, and D. E. Cowley. 2007. Estimation of introgression in cutthroat trout populations using microsatellites. Conservation Genetics 8:1311–1329.

Pritchard, J. K., M. Stephens, and P. Donelly. 2000. Inference of population structure using multilocus genotype data. Genetics 155:945–959.

Raymond, M., and F. Rousset. 1995. GENEPOP (version-1.2): population-genetics software for exact tests and ecumenicism. Journal of Heredity 86:248–249.

Reuterwall, C. 1980. Genetic variation in a large game species, the moose (Alces alces): patterns of differentiation and some management implications. Ph.D. dissertation, University of Stockholm, Sweden.

Reuterwall, C. 1981. Temporal and spatial variability of the calf sex-ratio in Scandinavian moose *Alces-alces*. Oikos 37:39–45.

Reynolds, J., B. S. Weir, and C. C. Cockerham. 1983. Estimation of the co-ancestry coefficient – basis for a short-term genetic-distance. Genetics 105:767–779.

Rousset, F. 2000. Genetic differentiation between individuals. Journal of Evolutionary Biology 13:58–62.

Ryman, N., G. Beckman, G. Bruun-Petersen, and C. Reuterwall. 1977. Variability of red cell enzymes and genetic implications of management policies in Scandinavian moose (*Alces alces*). Hereditas 85:157–162.

Ryman, N., C. Reuterwall, K. Nygren, and T. Nygren. 1980. Genetic variation and differentiation in Scandinavian moose (*Alces alces*): are large mammals monomorphic? Evolution 34:1037–1049.

Schmidt-Vogt, H. 1977. Die Fichte. Parey, Hamburg-Berlin.

Seddon, J. M., F. Santucci, N. J. Reeve, and G. M. Hewitt. 2002. Caucasus Mountains divide postulated postglacial colonization routes in the white-breasted hedgehog, *Erinaceus concolor*. Journal of Evolutionary Biology 15:463–467.

Slatkin, M. 1995. A measure of population subdivision based on microsatellite allele frequencies. Genetics 139:457–462.

Smouse, P. E., and R. Peakall. 1999. Spatial autocorrelation analysis of individual multiallele and multilocus genetic structure. Heredity 82:561–573.

Sokal, R. R., and N. L. Oden. 1978a. Spatial autocorrelation in biology. 1. Methodology. Biological Journal of the Linnean Society 10:199–228.

Sokal, R. R., and N. L. Oden. 1978b. Spatial autocorrelation in biology. 2. Some biological implications and four applications of evolutionary and ecological interest. Biological Journal of the Linnean Society 10:229–249.

Sokal, R. R., and D. E. Wartenberg. 1983. A test of spatial autocorrelation analysis using an isolation-by-distance model. Genetics 105:219–237.

Solberg, E. J., V. Grøtan, C. M. Rolandsen, H. Brøseth, and S. Brainerd. 2005. Change-in-sex-ratio as an estimator of population size for Norwegian moose. Wildl Biol 11:91–100. Ecography 27:677–687.

Solberg, E. J., et al. 2006. Elgen i Norge sett med jegerøyne. En anlyse av jaktmaterialet fra overvåkningsprogrammet for elg og det samlede sett elg-materialet for perioden 1996–2004. NONA Rapport 125 (in Norwegian). http://www.nina.no/archive/nina/PppBasePdf/rapport/2006/125.pdf. Accessed September 2015.

Spiegelhalter, S. D., N. G. Best, B. P. Carlin, and A. V. D. Linde. 2002. Bayesian measures of model complexity and fit. Journal of the Royal Statistical Society Series B – Statistical Methodology 64:583–639.

Strandgaard, S. 1982. Factors affecting the moose population in Sweden during the 20th century with special attention to silviculture. Report no 8 from the Department of Wildlife Ecology. Swedish University of Agricultural Sciences, Uppsala, Sweden.

Sumner, J., F. Rousset, A. Estoup, and C. Moritz. 2001. Neighbourhood size, dispersal and density estimates in the prickly forest skink (*Gnypetoscinus queenslandiae*) using individual genetic and demographic methods. Molecular Ecology 10:1917–1927.

Sweanor, P. Y., and F. Sandegren. 1988. Migratory behavious of related moose. Holoarctic Ecology 11:190–193.

Sweanor, P. Y., and F. Sandegren. 1989. Winter-range philopatry of seasonally migratory moose. Journal of Applied Ecology 26:25–33.

Swedish Association for Hunting and Wildlife Management (Svenska Jägareförbundet). 2008. Action plan för moose. Swedish Association for Hunting and Wildlife Management, Nyköping, Sweden.

Swedish EPA. 1982. Fauna management and hunting. Yearbook of the Swedish Environmental Protection Agency 1982. Stockholm, Sweden (in Swedish).

Szymura, J. M., D. H. Lunt, and G. M. Hewitt. 1996. The sequence and structure of the meadow grasshopper (*Chorthippus parallelus*) mitochondrial srRNA, ND2, COI, COII ATPase8 and 9 tRNA genes. Insect Molecular Biology 5:127–139.

Taberlet, P., and J. Bouvet. 1994. Mitochondrial-DNA polymorphism, phylogeography, and conservation genetics of the brown bear Ursus-arctos in Europe. Proceedings of the Royal Society of London, B. Biological Sciences 255:195–200.

TABERLET, P., L. FUMAGALLI, A. G. WUST-SAUCY, AND J. F. COSSON. 1998. Comparative phylogeography and postglacial colonization routes in Europe. Molecular Ecology 7:453–464.

TAJIMA, F. 1989. Statistical method for testing the neutral mutation hypothesis by DNA polymorphism. Genetics 123: 585–595.

TAMURA, K., G. STECHER, D. PETERSON, A. FILIPSKI, AND S. KUMAR. 2013. MEGA6: molecular evolutionary genetics analysis version 6.0. Molecular Biology and Evolution 30:2725–2729.

VAN OOSTERHOUT, C., W. F. HUTCHINSON, D. P M. WILLS, AND P. SHIPLEY. 2004. MICRO-CHECKER: software for identifying and correcting genotyping errors in microsatellite data. Molecular Ecology Notes 4:535–538.

WARTENBERG, D. 1989. SAAP: spatial autocorrelation analysis program. Exeter Software, New York.

WEIR, B. S. 1996. Genetic data analysis II: methods for discrete population genetic data. Sinauer, Sunderland, Massachusetts.

WRIGHT, S. 1946. Isolation by distance under diverse systems of mating. Genetics 31:39–59.

XENIKOUDAKIS, G., ET AL. 2015. Consequences of a demographic bottleneck on genetic structure and variation in the Scandinavian brown bear. Molecular Ecology 24:3441–3454.

Submitted 13 December 2014. Accepted 26 August 2015.

Associate Editor was Marjorie Matocq.